




Integration of geophysical, core and production data to evaluate gas reservoir performance: A study from Saldanadi field

MD ALIUR RAHMAN^{1,*} , MD AMIRUL ISLAM², JAHANGIR KABIR³,
A S DAIYAN AHMED², M NUR ALAM ZICO⁴ and MD YAMIN KHAN⁵

¹Department of Petroleum and Mining Engineering, Jashore University of Science and Technology, Jashore 7408, Bangladesh.

²Department of Petroleum and Mining Engineering, Military Institute of Science and Technology, Dhaka, Bangladesh.

³Reservoir and Data Management Division, Petrobangla, Dhaka, Bangladesh.

⁴Department of Petroleum and Mineral Resources Engineering, Bangladesh University of Engineering and Technology, Dhaka, Bangladesh.

⁵Department of Mechanical Engineering, Military Institute of Science and Technology, Dhaka, Bangladesh.

*Corresponding author. e-mail: a.rahman01@just.edu.bd

MS received 25 June 2023; revised 4 November 2023; accepted 7 November 2023

The present study offers a comprehensive, integrated assessment for characterising the Saldanadi gas reservoir, understanding its dynamic behaviour, and assessing its future development potential through simulation. The objective of this study is to develop an integrated 3D reservoir model and validate the static model through dynamic simulation. The Saldanadi reservoir has presented unique challenges from the outset, given its heterogeneity in petrophysical parameter distributions, encompassing the porosity, permeability, net-to-gross ratio, fluid saturation, and gas sand thickness. As a result, the field must be reassessed, and a reliable reservoir model must be developed for production forecasting. Utilising seismic data, wireline logs, drill stem tests (DSTs), and core data, we leveraged Petrel software to distribute reservoir parameters throughout the field, culminating in a 3D reservoir static model that was subsequently validated using the Eclipse reservoir simulator, with historical production data serving as a benchmark. Our updated reservoir model estimated gas initially in place at $149.63 \times 10^8 \text{ sm}^3$, considering four potential gas sands. The historical production profile was reviewed to determine the reservoir's performance and dynamic characteristics, and forecasts were made accordingly. Our study suggests that the validated model will serve as the guiding constraint for future development strategies and the pursuit of an optimal recovery factor.

Keywords. Integrated reservoir modelling; reservoir heterogeneity; dynamic simulation; reservoir model validation; historical matching.

1. Introduction

Integrated reservoir modelling plays a crucial role in simulation studies and future reservoir development plans (Ganguli *et al.* 2016; Ganguli and Sen

2020; Ali *et al.* 2022). This modelling approach offers the advantage of evaluating both structural and petrophysical aspects by integrating seismic sections and well control systems. The geological features in software such as Petrel seamlessly

integrate with geophysical and reservoir engineering tools, facilitating comprehensive studies for precise static reservoir representations (Abdel-Fattah *et al.* 2010). Consequently, the development of a reservoir model is a key component of overall reservoir management. Utilising integrated geological, geophysical, petrophysical, geostatistical, and reservoir engineering methods enhances reservoir characterisation (Ganguli *et al.* 2018; Baouche *et al.* 2020), which is essential for predicting reservoir performance and production indicators (Ganguli 2017; Sen *et al.* 2021). Numerous global studies have been conducted on static and dynamic reservoir modelling (Cunha 2003; Alao *et al.* 2013; Amigun and Bakare 2013; Adeoti *et al.* 2014; Ilozobhie and Egu 2019; Ahmad *et al.* 2021; Okoli *et al.* 2021).

In 1996, Bangladesh Petroleum Exploration and Production Company Limited (BAPEX) made a significant discovery in the Saldanadi gas field, which is part of the larger Rukhia anticline in the Bengal basin. During the drilling of Saldanadi well-1 (SLD #1), two gas sands were discovered and completed as dual producers by the Bangladesh Oil, Gas, and Mineral Corporation (Petrobangla) in 2004. In 1999, Saldanadi well-2 (SLD #2) was drilled to appraise the structure and encountered another gas sand layer, which was completed as a single producer. Subsequently, two more wells were drilled: Saldanadi well-3 (SLD #3) and Saldanadi well-4 (SLD #4). However, SLD #1 and SLD #2 ceased production in 2012 due to declining production rates, tubing head pressure, and water production. Currently, only SLD #3 and SLD #4 are producing at reduced rates, with production rates of approximately 19,821 and 3,275 sm³/d and wellhead pressures of 33.79 and 33.10 bar, respectively (Bangladesh Oil 2023). Therefore, a review of the gas reservoir and the development of a validated reservoir model are necessary for future production predictions. Several studies have been conducted in this field in the past, with the last simulation performed in 2009 by RPS Energy Consultants Limited (RPS). Dynamic reservoir analysis, from individual wells to the entire gas field, is essential for optimising development strategies and production frameworks (Shang *et al.* 2021). Previous investigations identified three gas sand units, including upper gas sand (UGS), middle gas sand (MGS), and lower gas sand (LGS). However, in this research, four potential gas sands are identified through the integration of seismic data, well-log interpretation, and synthetic seismogram analysis in the Saldanadi gas field. Many other reservoir models

have been developed for petrophysical property evaluation, characterisation, and reservoir performance monitoring (Du *et al.* 2009; Nabawy and Shehata 2015; Soleimani and Jodeiri Shokri 2015; Abd El-Gawad *et al.* 2019; Adelu *et al.* 2019; Amanipoor 2019; Elsheikh *et al.* 2021; Ebong *et al.* 2021; Rao *et al.* 2021; Sharifi *et al.* 2021; Li *et al.* 2023).

In this study, a 3D reservoir model is constructed using PetrelTM software, which is Schlumberger's reservoir modelling software, by integrating interpreted seismic sections, wireline logs, and core data. We employed the best-adjusted parameters for reservoir simulation to reduce static model uncertainties. The 3D reservoir static model is validated through production and pressure history matching with simulated modelling, providing valuable insights for future hydrocarbon exploration (Sallam *et al.* 2015). An objective function measures the difference between observed and simulated values, which is subsequently integrated into the reservoir model's design (Mirzadeh *et al.* 2014). This research aims to build a valid 3D reservoir model, characterise the reservoir, and simulate its performance.

1.1 Stratigraphy

The sediments comprising the area are poorly fossiliferous to barren and consist of different proportions of alternating shales, sandstones, and siltstones. The regional tectonic map of the study area is shown in figure 2(c). The sedimentary strata encountered in the Saldanadi gas field are alluvium, the Tipam Sandstone, the Bokabil Formation, and the Bhuban Formation (Bangladesh Petroleum Exploration 2004). The Tipam Sandstone consists mainly of loose quartz sand, which is clear to white, medium to very fine-grained, and poorly sorted. The section is locally interbedded with silt or siltstone; towards the base, the sand grains become fine to very fine. The Bokabil formation consists mainly of sandstones, shales, and siltstones. According to the references (Bapex 2001a; Bangladesh Petroleum Exploration 2004; Bangladesh Oil 2009b) of SLD #1 and SLD #2, the following stratigraphic succession has been outlined in response to the depth of penetration shown in table 1.

1.2 Petroleum system

The hydrocarbon source is the Miocene Bhuban shale, which has released mostly natural gas and

very little condensate (Bangladesh Oil 2009c). Elongated anticlines trending almost NW–SE are the trap type in the field. This compressional structuring occurred from the Miocene to the present. The total organic carbon contents have average values of 0.2–0.7% (Bangladesh Oil 2009a). The upper marine shale and intraformational seal are identified from the well and seismic section, respectively. In the Saldanadi reservoir, most of the gas is probably sourced from shaly sections. The reservoir rock in that area is mostly sandstone of the Bokabil and Upper Bhuban formations, with porosities ranging from 15 to 21% and permeabilities in the range of 116–193 mD (Bangladesh Oil 2009a).

1.3 Background of the study area

Since the discovery of the Saldanadi gas field, several studies have been conducted on it. The estimated total gas initially in place (GIIP) of the Saldanadi gas field is 165.80 Bcf, of which 116.03 Bcf is recoverable gas (Bapex 2001b). In 2009, the RPS energy report revealed that the GIIP volume estimated at 379.9 Bcf from the simulation model (ECLIPSETM) is consistent with the values from the volumetric calculations performed in PetrelTM

and REPTM (Bangladesh Oil 2009c), but no historical matching has been established. The measured tubing head pressure (THP) and a few shut-in periods in well SLD #1 in both upper and lower sand indicate no measured static bottomhole pressure (BHP) data. However, a few static BHP values have been estimated from the measured THP at the end of each shut-in period (Bangladesh Oil 2009c); these estimated static BHP data are not entirely reliable, and downhole-measured data are the most dependable. The cumulative gas initially in place (GIIP) for both upper and lower gas sand is 501.166 Bcf, of which 350.83 Bcf can be recovered at a rate of 70% (Dey *et al.* 2016).

2. Methodology and materials

The primary objectives of this simulation are to characterise the reservoir and assess its performance. To achieve this, the ideal combination of settings for the reservoir is determined by observing the model’s performance under various operating conditions. This includes defining the number of space/grid dimensions, modelling the fluid and rock properties of the reservoir, and establishing the relationships between the wells and the reservoir.

Table 1. Stratigraphic succession of the study area modified after previous studies (Bapex 2001a; Bangladesh Petroleum Exploration 2004; Bangladesh Oil 2009a).

Age	Formation	Depth (m)	Lithological description
Quaternary	Alluvium	Surface–50	Dominantly sand with alluvial cover.
Pliocene	Tipam sandstone	50–530	Predominantly sandstone, interbedded with clay and siltstone and traces of lignite.
	Bokabil	530–1140	Predominantly sandstone with alterations of shale and siltstone. Sandstone is mainly white, clear, massive, loose, occasionally consolidated, and fine- to medium-grained, moderately sorted, with dark minerals that are concentrated, and it is occasionally calcareous.
Miocene	Bhuban	1140–1300	Shale dominates with alterations of sandstone and siltstone. Shale is mainly light grey to dark grey, thinly laminated, hard and compact, and slightly calcareous with silt partings.
		1300–2070	Alternations of sandstone and shale. Predominantly white, clear, and transparent sandstone. Fine- to medium-grained, unconsolidated, subrounded, moderately sorted, with concentrated mica and dark minerals, and occasionally calcareous.
		2070–2170	Predominantly shale, grey and bluish-grey in colour, and thinly laminated.
		2170–2215	Predominantly sandstone that is light, white, and coarse. This sand is gas-saturated.
		2215–2405	Predominantly shale, bluish grey in colour that is very thinly laminated, moderately hard and compact, silty in nature, and mildly calcareous.
		2405–2511	The upper part is dominantly sand, and this sand is gas-saturated. The lower part is a shaly sequence with minor sandstone.

The initial step in this process involves creating a reservoir geological model, commonly called a static model. The static model portrays the reservoir's fluids in a static state without considering fluid flow within the reservoir or the production and injection of fluids through the wells. Subsequently, the static model is imported into the simulation, and the fluid flow phenomenon is incorporated in the second phase, utilising Darcy's law. This is accomplished by modifying the static model and adding additional data, such as fluid characteristics, injection rates, production rates, and other pertinent parameters.

The construction and operation of a model replicating a real reservoir's behaviour are integral to simulating petroleum reservoir performance. The primary goal of this study is to develop a reliable reservoir model, validate the static model through historical production and pressure data matching, and make production forecasts accordingly. In this study, we employ Petrel software to construct the reservoir model, while the history-matching process is carried out using the 3D black oil reservoir simulator ECLIPSE. The workflow is illustrated in figure 1.

2.1 Datasets used

The quality of the data is variable, ranging from medium to good. Digital well log data and 2D seismic data are used, with the well log data in LAS format and the seismic data in SEG-Y format. All other types of data, such as wellhead data, gas-water contact data, and velocity data, are given in ASCII format. To initiate the project, a database file is created and initialised. All of the well log data are loaded into PetrelTM in text and LAS formats. The log curves contained in the database are checked against the original logs to ensure that the data are correct. The missing log curves have been digitised from hard copies since the digitising tool became available. Six conventional cores are cut from both the shale and sandstone of SLD #1 to study the physical properties of the rock, such as the porosity, permeability, reservoir parameters, age, and depositional environment.

2.1.1 Seismic and wellhead data

Seismic interpretation of the Saldanadi structure is performed using Petrel software. All seismic

interpretation and structure maps, including time and depth maps, are created with the SEG-Y data format. Wellhead data are prepared according to the format by including the name, Y (northing), X (easting), Kelley Bushing (KB), and total depth (TD) of the measured depth (MD) of the wells. Wellhead data are created in an Excel sheet, Notepad, or WordPad and imported in wellhead format. SLD #1 is a vertical well, while SLD #2, SLD #3, and SLD #4 have deviated wells. Therefore, to locate these wells accurately on the map, deviated well data are needed. The deviated well data include the measured depth (MD), inclination azimuth, etc. These data are input into an Excel sheet and then saved in Notepad or WordPad in text format. Deviated data are arranged according to the needed format and imported into the model to transform the deviated well data into the well path/deviation (ASCII) format.

2.1.2 Wireline log data

Conventional wireline log data that are available for the study include calliper, gamma ray, resistivity (deep, medium, and shallow), micro-resistivity, sonic log, neutron log, density log, facies log, self-potential (SP) log data, etc. All these data are input into Notepad or Excel sheets and Petrel software. These logs are imported in LAS format. These data are used for correlation from well to well and also for other purposes. The available conventional logs stated earlier are interpreted in Petrel software, and the clay content, porosity, permeability, and water saturation are calculated. These properties, together with the conventional logs, are imported into Petrel in 'well log ASCII' format. Using the cross-plot of analyses of well log data, potential hydrocarbon-bearing zones are identified (Khan and Rehman 2019; Ehsan and Gu 2020; Babu *et al.* 2022).

2.2 Seismic interpretation

The major aspect of hydrocarbon potential zone identification and the development strategy is seismic interpretation (Adeoti *et al.* 2014; Naseer 2023). Eleven seismic lines are interpreted using Petrel interpretation software (figures 2a and b). Using the available checkshot data, a project is made to analyse these seismic lines and construct the time and depth contour maps of the field. The

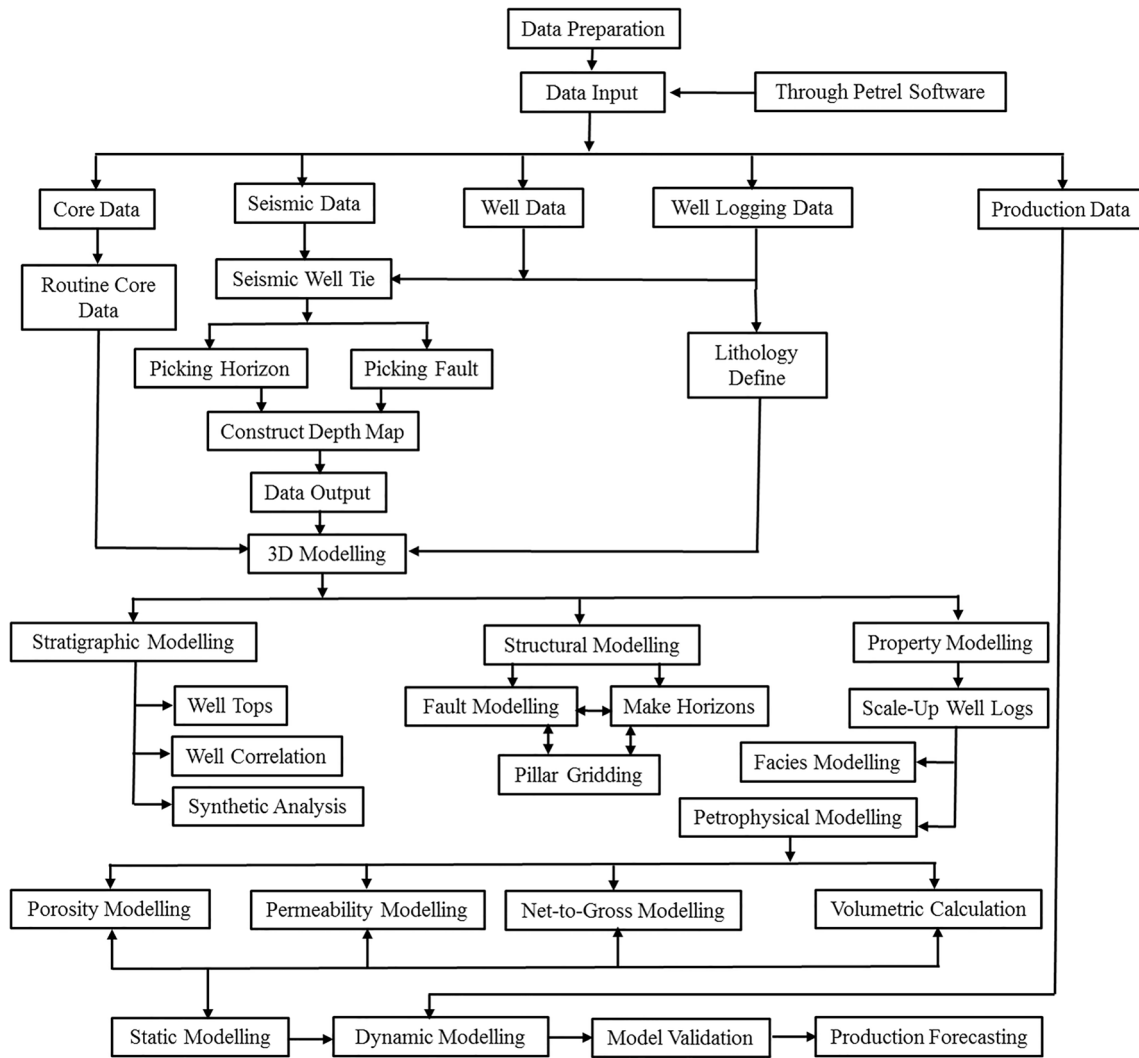


Figure 1. Workflow adopted for the study.

two types of interpretation processes used in this research work are as follows: (i) time-to-depth conversion using the T–Z curve and (ii) interpretation of seismic lines and velocity data from the SLD #1 well. With all these data, a time distance (T–Z) curve is created, which is useful for seismic line interpretation. According to Qadri *et al.* (2017), to convert the two-way travel time (TWT) into depth, the average velocity of the well with corrected checkshot data is considered.

2.3 Performing seismic-to-well ties

A synthetic seismogram analysis attempts to identify the hydrocarbon-promising zone using the integration of seismic sections and digital well log interpretation (figure 3a). The information is used

to link seismic data to well data in this investigation (Rahimi and Riahi 2020). Synthetic seismogram analysis is conducted between SLD #1 with gamma-ray logs and the survey line of SD 07 of the seismic section. Here, gas-bearing sandstone zones are identified by matching the gamma-ray log response and seismic reflection peak (figure 3a). The continuity of seismic reflection is also considered. To determine well tops and bases, NGS 2, NGS 1, UGS, and LGS horizons are picked by manual interpretation of the seismic horizons of different seismic sections by correlating well logs. From synthetic seismogram analysis, we attempt to determine the HC zone of interest and find an excellent correlation between the seismic and well log sections. As a result, four potential hydrocarbon zones are identified.

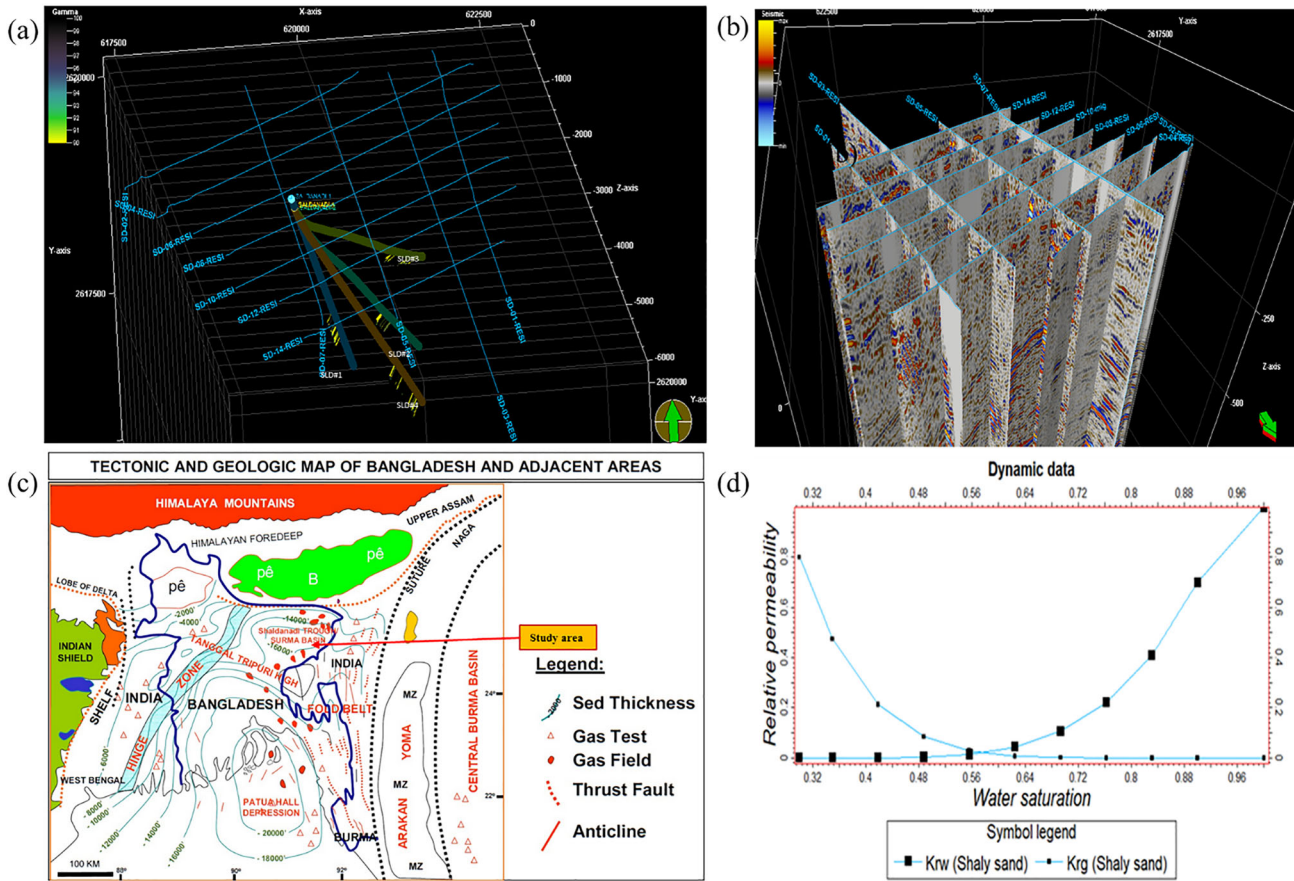


Figure 2. (a) 2D seismic lines from four wells, (b) eleven seismic lines in 3D view, (c) regional tectonic map of the study area (Bangladesh Petroleum Exploration 2004), and (d) relative gas–water permeability.

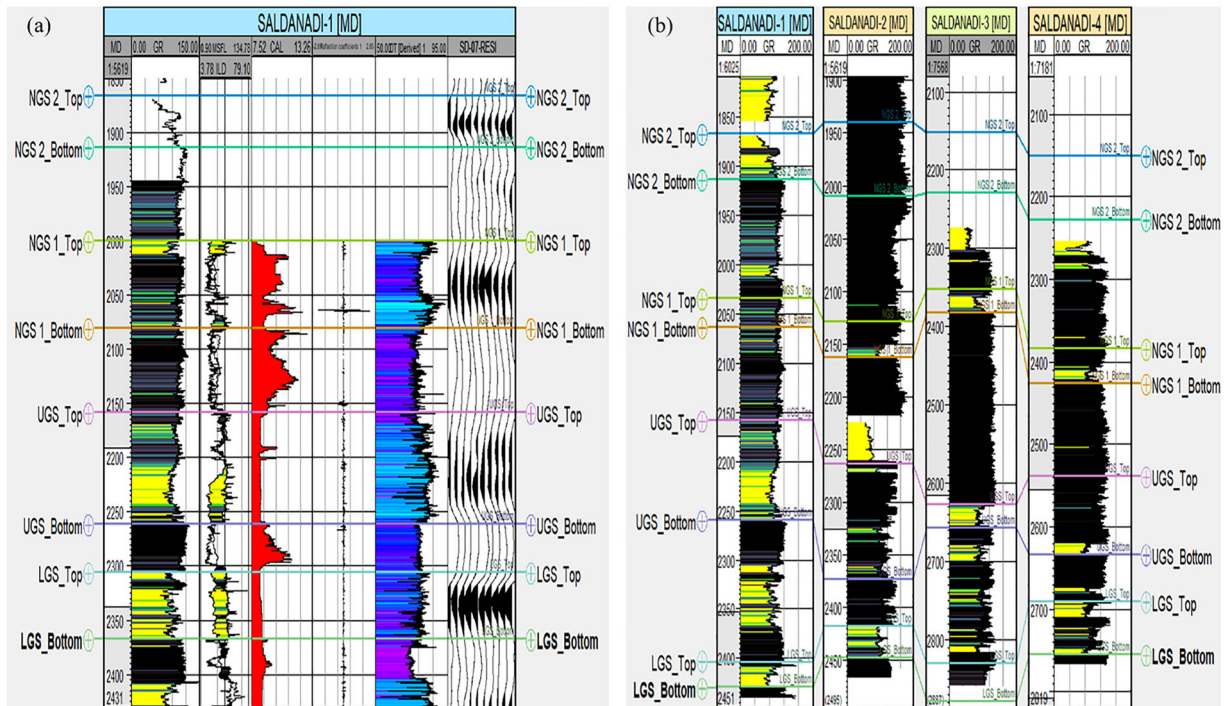


Figure 3. (a) Synthetic seismogram analysis and (b) well-to-well correlation.

2.4 Fault modelling and horizon construction

No fault is observed from the available 2D seismic data at the Saldanadi structure and its vicinity. However, there have been reports of a fault delineated on the surface topography map at the eastern flank. This is probably because the low resolution of 2D seismic data likely causes fewer fault sightings, but a high-resolution 3D dataset should reveal more features (Bangladesh Oil 2009b). Fault modelling and pillar modelling are performed using interpreted fault line picking for subsurface structure modelling purposes. The seismic grid and depth maps imported in Petrel are converted into surfaces using the make/edit surface option in the 'Make Horizon Process'. Desired top and base horizons of the respective gas sands from the wells are taken for analysis and attributes (Khan *et al.* 2023). Interpreted horizons are employed in model-based seismic inversion techniques to determine the geographical distribution of porosity (Toqeer *et al.* 2021).

2.5 Zone-making and layering

The zone-making process is used to make zones. Depth maps along the tops and bases are converted into surfaces and used as input for zone-making. The zones are built from the top horizon along the stratigraphic thickness where tops and bases lie as conformable in the model. Artificial layers are created using proportional thicknesses for NGS 2, NGS 1, UGS, and LGS and are corrected later according to the vertical range of the facies. NGS 2 and NGS 1 are subdivided into 5–11 artificial layers, with an average thickness of 10.2 m. UGS and LGS, on the other hand, are subdivided into 12–24 layers, with an average thickness of 9.5 m. This layering results in a grid block dimension ($70 \times 44 \times 23$) of cells, and the total number of 2D nodes is 2475.

2.6 Well correlation

The reservoir succession is divided into four main zones: New Gas Sand 2 (NGS 2), New Gas Sand 1 (NGS 1), Upper Gas Sand (UGS), and Lower Gas Sand (LGS); each is separated by a well-developed shale section that can be correlated across the field. Zone UGS is the thickest of the four and provides the most laterally extensive and productive reservoirs in the field. Four gas-bearing horizons are

encountered in all the wells. The reservoir tops of NGS 2, NGS 1, UGS, and LGS are correlated using well logs, and the depth interval is shown in figure 3(b).

2.7 Well-completion design

Well-completion design is the strategy used to maximise HC production and the well lifetime by tuning various parameters, such as perforation placement, tubing, and skin effects. Designing corresponding wells is necessary before undertaking dynamic simulation and matching historical production data. As in this study, the historical match is based on surface production data, but reservoir production is not determined. We model the vertical flow performance (VFP) of the well. The output of the reservoir flow rate and pressure is converted to surface production by the lift curve. Well design and completion are important in this step to ensure the dynamic simulation's accuracy, net pay thickness, perforation position, and tube size. According to the specifications in Petrobangla (2016), the well-completion designs of Saldanadi wells 1, 2, 3, and 4 are arranged in figure 4. Among all four gas sand units, the upper gas sand is the thickest gas sand. Perforation is conducted in UGS and LGS in SLD #1 and in UGS in SLD #2. Additionally, perforation is conducted in NGS 2 and NGS 1 in SLD #3 and in UGS and LGS in SLD #4.

2.8 Geological model construction

The structural map, well-log data, and core analysis data are used to build the geological model. The dynamic model is acquired after making the necessary adjustments. The simulation is carried out to identify historical correlations. A most likely model is built for the Saldanadi field to estimate the GIIP and generate input for the reservoir simulation model that is applied to formulate the depletion behaviour and reservoir management plan for the field. The model integrates seismic interpretation, petrophysical data, and well data. The structural and stratigraphic modelling of the reservoirs is conducted using the seismic depth grids of the tops of the main four reservoir sand units: NGS 2, NGS 1, UGS, and LGS. The grid is built using a 100×100 m grid spacing, which results in grid dimensions of $70 \times 44 \times 23$ (x, y, z) to represent the four distinct gas sands

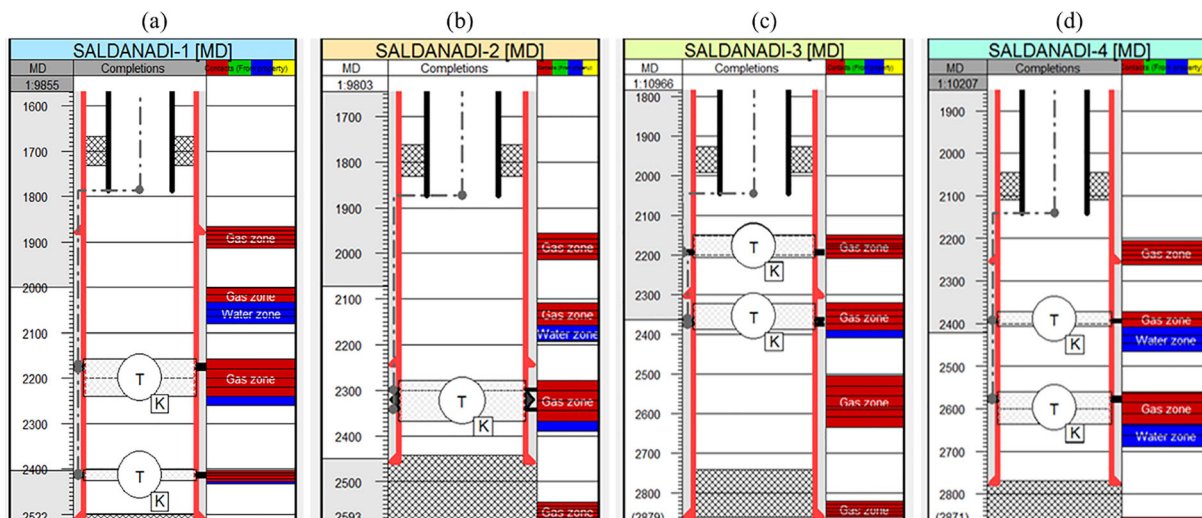


Figure 4. Well completion design of (a) SLD #1, (b) SLD #2, (c) SLD #3, and (d) SLD #4.

Table 2. Layering of the grid model of the reservoir.

Sl. no.	Horizon		Simulation layer	Status
1	New Gas Sand 2	NGS 2	1–5	Active
	Interlayer	–	6	Inactive
2	New Gas Sand 1	NGS 1	7–11	Active
	Interlayer	–	12	Inactive
3	Upper Gas Sand	UGS	13–17	Active
	Interlayer	–	18	Inactive
4	Lower Gas Sand	LGS	19–23	Active

encountered in the field, with a total of 70,840 cells. A thick, continuous shale interlayer separates the three gas sands from each other, resulting in no vertical communication between the zones. The model grid layering is presented in table 2.

2.9 Relative permeability and capillary pressure

The Saldanadi gas field has no special core analysis (SCAL) data. Thus, relative permeability curves (figure 2d) are produced for the simulation using the Brooks–Corey correlation for two-phase flow (Abdelmaksoud and Radwan 2022). The average value of the available capillary pressure data from different fields of the Surma basin is thought to be the capillary pressure of water. Therefore, this water distribution is followed in the initial equilibration, and the initial water distribution is used to scale the gas–water capillary pressure curves. The initial water saturation data show no clear evidence of a transition zone. This does not necessarily imply that the wells will not experience any capillary effects during production. The completion of the well in the upper sand

is more than 100 feet above the gas–water contact encountered in the sand. The water production history of the wells also suggests that no aquifer water has been produced, so there is either no transition zone or, if there is, the impact is insignificant.

2.10 Structure

The construction of a structural model gives us visualisation for new well trajectories and tests the model via structural sections, volumetric calculations, and reservoir simulation grids. No faults were found from the manual interpretation of 2D seismic data (Faleide *et al.* 2021), but some faults can be visualised in a 3D seismic survey. These faults do not have a significant impact on reservoir connectivity or productivity. In this study, geometry captured via seismic structure contour maps (Khan *et al.* 2019) is constructed for the field to illustrate the subsurface structure. During 3D structural modelling, the seismic interpretations are taken as the main input (Ali *et al.* 2022), and the depth structure map is also made.

2.11 Property modelling

Property modelling is the main step in modelling porosity, permeability, and facies between the wells and the model. It includes geometrical modelling, scale-up well logs, facies modelling, and petrophysical modelling. These steps are followed during the modelling process and described successively. Geometrical properties such as cell height, bulk volume, and zones (hierarchy) have been modelled in this process according to the needed method. The main purpose of geometrical modelling is to calculate the bulk volume, pore volume, etc. Scaling-up means averaging log values in a cell. The log values are distributed by considering cell values in the model. In this step, both discrete (facies) and continuous properties (porosity, permeability, etc.) are averaged in each grid cell along the well path. The lateral and vertical heterogeneities in reservoir facies distribution are established from reservoir characterisation and directly impact hydrocarbon reserve estimation (Ehsan *et al.* 2021; Narayan *et al.* 2023). Depending on whether a property is discrete or continuous, different tools and methods are available within the data analysis process window (Vo Thanh and Lee 2022). Before facies and petrophysical modelling, data analysis must be performed. In the Saldanadi model, both discrete and continuous data analyses are performed based on available log data from four wells with variogram plotting.

2.12 Petrophysical modelling

Petrophysical simulation is performed using sequential Gaussian simulation (SGS) with the integration of seismic data, well logging signatures, analysed core data, drill stem tests (DSTs), and the results of the petrophysical property assessment of various wells (Amanipoor 2019). The upscaling of well logs, input distribution, and variogram creation are the main inputs for petrophysical modelling to ensure petrophysical features (Mukherjee and Sain 2019; Abdelmaksoud and Radwan 2022). Petrophysical modelling consists of facies, porosity, permeability, and net-to-gross modelling and is described as follows.

2.12.1 Porosity modelling

The simulation model maintained the porosity of the geological model. Figure 5 illustrates how the porosity distribution fluctuates aerially by

displaying the porosity distribution of NGS 2, NGS 1, UGS, and LGS in the field. The porosity values of the analysed sandstone range from 13.72 to 28.85. It is noticeable that the majority of cells have an average porosity of approximately 16.61%.

2.12.2 Permeability modelling

The geological model's horizontal permeability is dispersed based on log data. When these data are entered into Eclipse, the highest value of permeability is discovered to be approximately 592 mD. The sandstone that has been studied has a permeability range of 60–240 mD. Using results from the core analysis, an average permeability of 192.40 mD is used for these four sands. The obtained data can be rated as having porosity and permeability in the moderate to fair range. Figure 6 shows the permeability distribution of NGS 2, NGS 1, UGS, and LGS in the X direction. Similarly, the permeability distribution model of all four gas sands is constructed in the Y and Z directions.

2.12.3 Facies and NTG modelling

The assigned values are loaded into a unique code for the lithology distribution to build the 3D facies model (Othman *et al.* 2021; Narayan *et al.* 2023). The stochastic sequential indicator simulation (SIS) method is also used to apply the 3D facies model (Ali *et al.* 2022). The log is upscaled later in the 'scaled-up well log' process. Variograms are used as input for facies modelling and the anisotropy of facies distribution (Orellana *et al.* 2014). The total pay footage divided by the total thickness of the reservoir interval yields the net-to-gross ratio. The net-to-gross (NTG) ratio is analysed to define productive zones and extract hydrocarbons.

2.12.4 Fluid distribution

The quantity of fluid contained in the pores expressed as a percentage of V_p is known as fluid saturation. Figure 7 depicts the fluid distribution (gas and water) model of NGS 2, NGS 1, UGS, and LGS of the Saldanadi gas field, where the 3D domal structures of the red portion indicate the gas saturation (Saravanavel *et al.* 2019) and the blue colour indicates the distribution of the water saturation throughout the gas sand area.

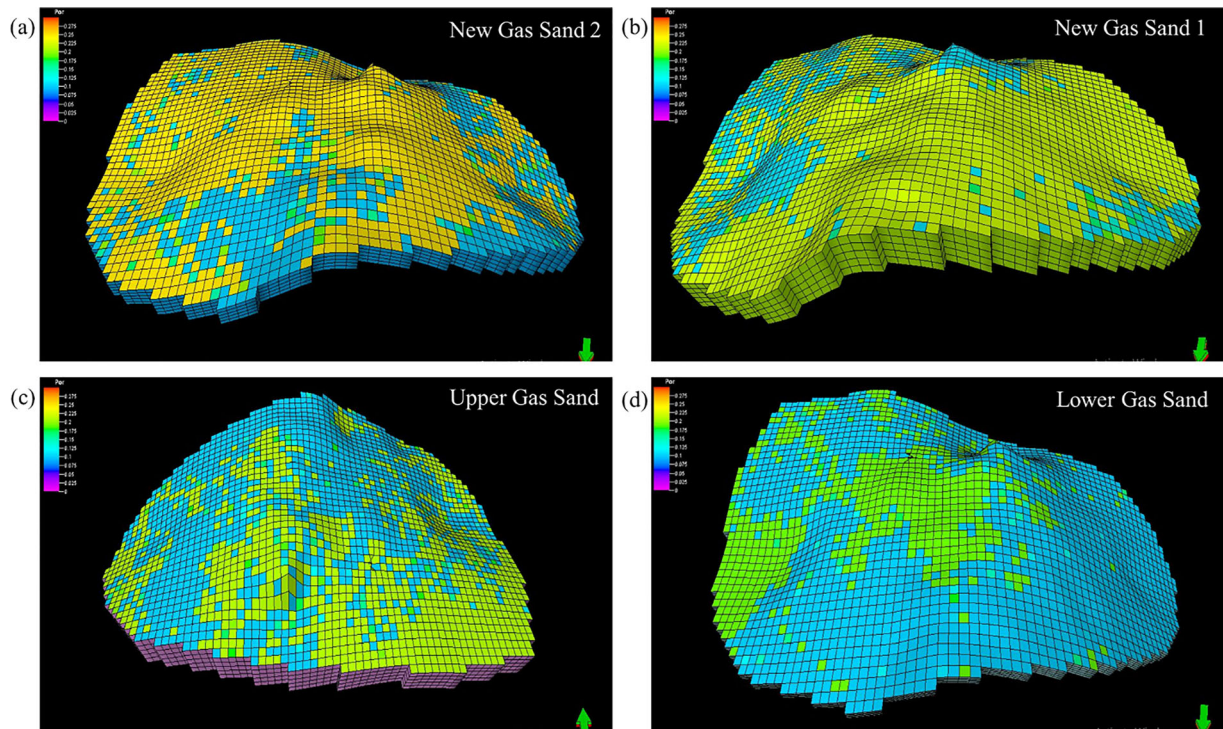


Figure 5. Porosity distribution model of (a) NGS 2, (b) NGS 1, (c) UGS, and (d) LGS.

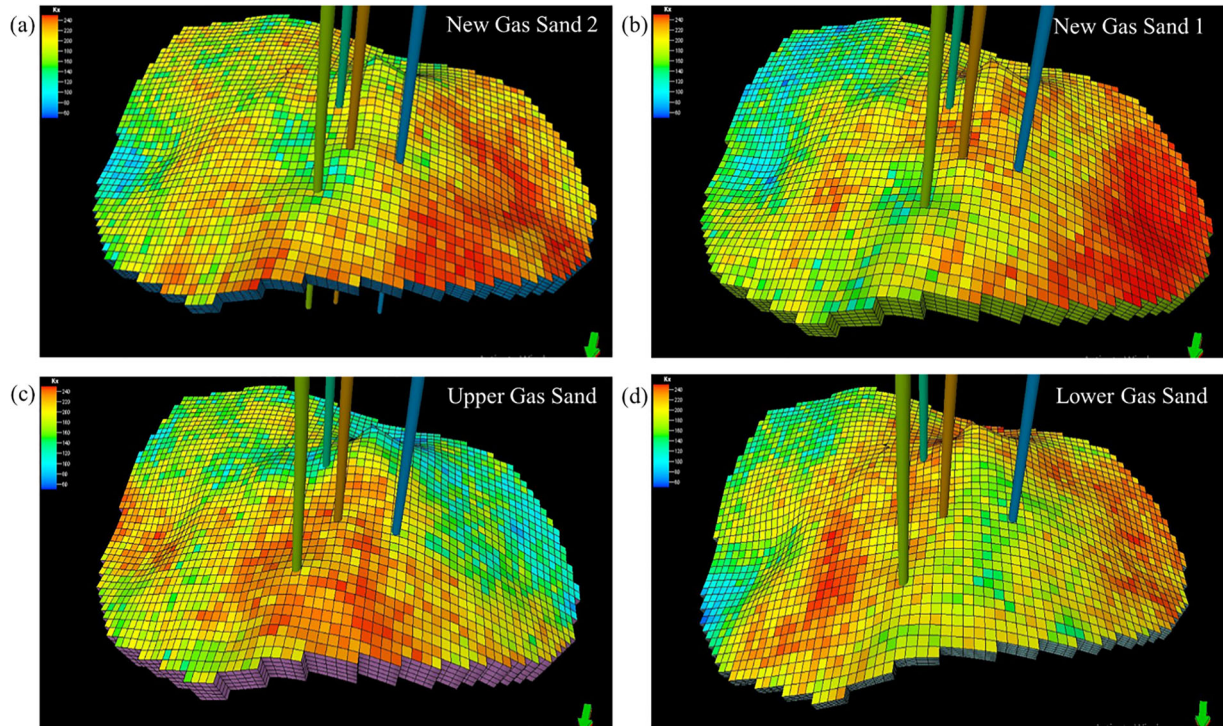


Figure 6. Permeability distribution of (a) NGS 2, (b) NGS 1, (c) UGS, and (d) LGS (X direction).

3. Model validation by historical matching

The previous section detailed the available data and the development of the simulation model. Unfortunately, bottomhole pressure data are not accessible. To address this limitation, we rely on wellbore schematics and wellhead pressure data from wells to fine-tune the multiphase flow correlation and estimate the bottom-hole pressures. We then generate vertical flow performance curves by varying wellhead pressures and estimating production rates. This process helps us gain insights into reservoir behaviour.

For this study, we conduct a PVT black oil simulation to predict the behaviour of reservoir fluids, a critical aspect of effective reservoir management. In our model, the reservoir fluid is characterised as dry gas, existing as a single phase under depletion conditions. Gas samples from four sets are collected from wells SLD #1 and SLD #2 at the surface (separator) during drill stem tests, and laboratory tests conducted by BAPEX are used to define the fluid properties for this reservoir simulation (table 3).

The reservoir conditions that are considered are a minimum pressure of 38 bar, a maximum pressure of 300 bar, a temperature of 190°F, and a reference pressure of 250 bar. These conditions,

along with the PVT properties, formation volume factor, and fluid viscosity, serve as inputs for the simulation model, encompassing the four gas sands. These PVT properties are consistent for all four gas sands, offering valuable insights into the design of reservoir depletion processes.

3.1 Gas rate match

Saldanadi well-1 has been producing from 1998 to 2012, and the cumulative production is $10.64 \times 10^8 \text{ sm}^3$. Production increased after a workover operation in SLD #1 in 2002. Wells SLD #1 and SLD #2 stopped their production in 2012 due to excessive water production, skin effects within the tubing, and formation damage. The first peak production of SLD #3 was approximately $42.47 \times 10^4 \text{ sm}^3$, which was sustained for two years. Then, the production rate declined continuously to July 2021. The graph also displays the total production of each individual well. Good historical matches are observed in all the wells, which indicates that the wells are controlled by the gas rate in the simulator (figure 8). Initially, the peak production of SLD #4, approximately $50.96 \times 10^4 \text{ sm}^3$, was sustained for two years. Then, the production rate showed a continuous up-and-down trend until July 2021. Then, forecasting started and continues from

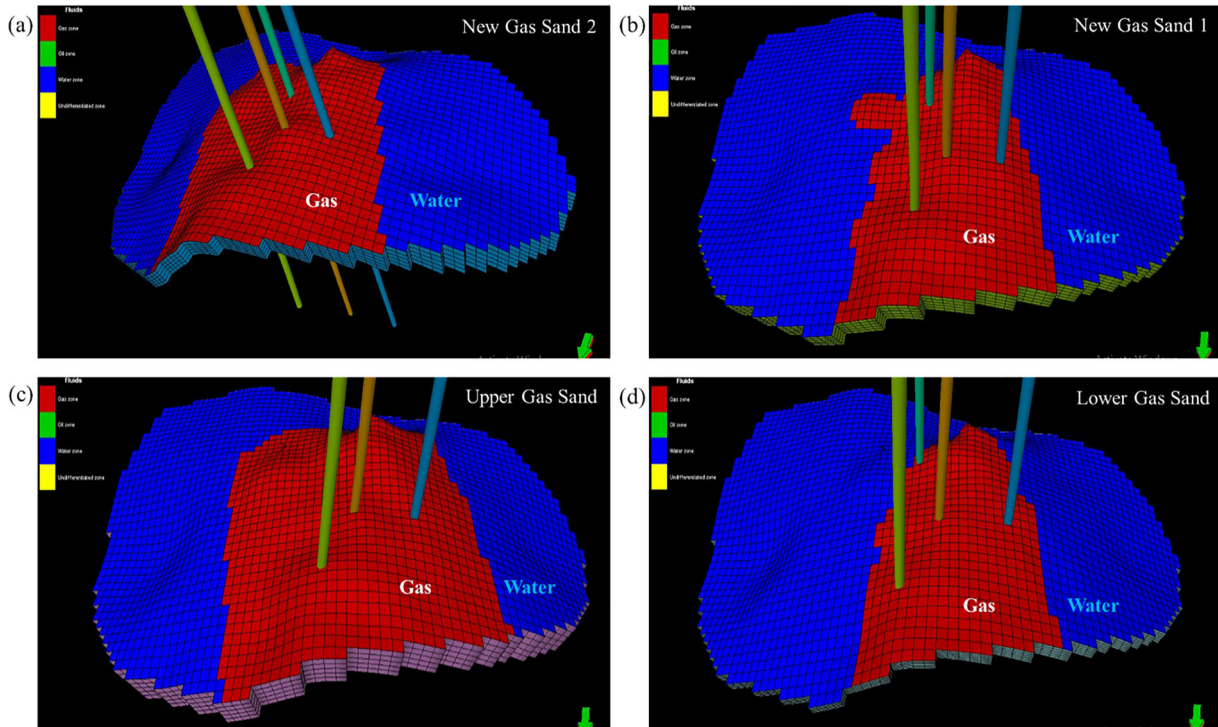


Figure 7. Fluid distribution (gas and water) of (a) NGS 2, (b) NGS 1, (c) UGS, and (d) LGS.

Table 3. PVT data of the reservoir fluid used in the simulation (Bangladesh Petroleum Exploration 2004; Bangladesh Oil 2009c).

Component	Mol (%)	Specific gravity	Pressure (bar)	Gas Formation volume (rm ³ /sm ³)	Gas viscosity (cP)
Methane (C ₁)	0.9632	0.562	38.0	0.042	0.016
Ethane (C ₂)	0.0216		64.2	0.025	0.017
Propane (C ₃)	0.0045		90.4	0.018	0.017
Butane (C ₄)	0.0012		116.6	0.014	0.017
Iso-butane (IC ₄)	0.0007		142.8	0.011	0.018
Normal butane (NC ₄)	0.0003		169.0	0.010	0.018
Iso-pentane (IC ₅)	0.0002		195.2	0.008	0.019
Normal pentane (NC ₅)	0.9632		221.4	0.007	0.019
Carbon dioxide (CO ₂)	0.0056		247.6	0.007	0.019
Nitrogen (N ₂)	0.0027		273.8	0.006	0.020

August 2021 to 2030, with a declining production of 3.96×10^4 sm³. The simulation indicates that the production of this well will be stopped at the end of 2024, maintaining the shutting pressure at 2.07 bar. At present, the production rates of the SLD #3 and SLD #4 wells are approximately 19,821 and 3,275 sm³/d, respectively (Bangladesh Oil 2023).

3.2 Pressure history matching

In the initial stage of history matching, regional pressures and pressure gradients are adjusted. The aquifer connection, reservoir permeability depth product (kh), transmissibility across faults, and regional pore volume are the matching characteristics that are the most frequently employed to match the pressure and pressure gradients. Changes in the regional pore volume and aquifer connectivity may have an impact on the match with the average reservoir pressure, necessitating a revision of the match with the average reservoir pressure. Figure 9 demonstrates the pressure distribution of the observed data with a simulated pressure profile. The pressure profile of all four wells reveals perfect matching at the initial stage, but later on, it is slightly deviated because of scaling formation within the tubing and formation damage. In Saldanadi-1, the pressure profile matched initially, and in 2002, a workover was conducted, and the pressure profile matched again, as there was no wax formation or tortuosity within the tubing. The simulation indicates that the production of this well will be stopped at the end of 2024. Currently, the wellhead pressures of the SLD #3 and SLD #4 wells are 33.79 and 33.10 bar, respectively (Bangladesh Oil 2023).

4. Results and discussion

A three-dimensional static reservoir model is constructed by integrating seismic data, well logs, core samples, well tests, and production data. Given that this reservoir is characterised as a dry gas reservoir with a single phase present, it is standard practice to use a black oil simulation. The primary purpose of this reservoir model is to investigate the reservoir's potential structure, rock properties, and fluid properties to estimate the volume of hydrocarbons. The dynamic modelling component aims to predict reservoir production performance, providing valuable insights for reservoir management.

4.1 Petrophysical parameters

We identified four dominant reservoir intervals: NGS 2, NGS 1, UGS, and LGS (table 4). These reservoirs exhibit typical porosities ranging from 13.5% to 28.5% and 60 to 240 mD permeabilities. The mean porosity and mean permeability across these reservoirs are approximately 16.61% and 192.02 mD, respectively. The net-to-gross (NTG) values vary from 0.6 to 1. Hydrocarbon saturation values range from 26% to 63.7%, while water saturation values range from 36.3% to 74%.

4.2 Gas–water contact

The gas–water contacts (GWCs) for NGS 2, NGS 1, UGS, and LGS have been interpreted from the logs. The GWC is observed at varying true vertical depth subsea (TVDSS) readings of 1897 m in NGS 2, 2021 m in NGS 1, 2215 m in UGS, and 2411 m in LGS (table 5).

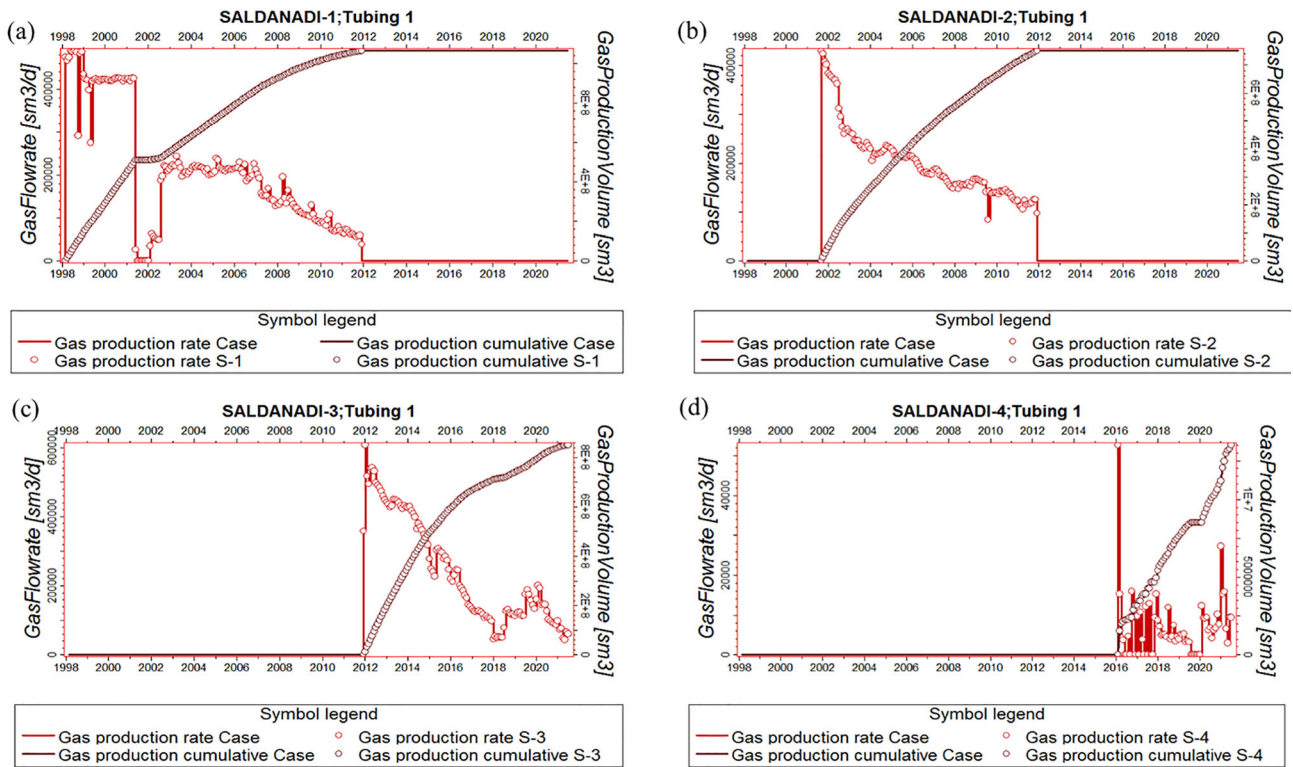


Figure 8. Gas rate historical match (a) SLD #1, (b) SLD #2, (c) SLD #3, and (d) SLD #4.

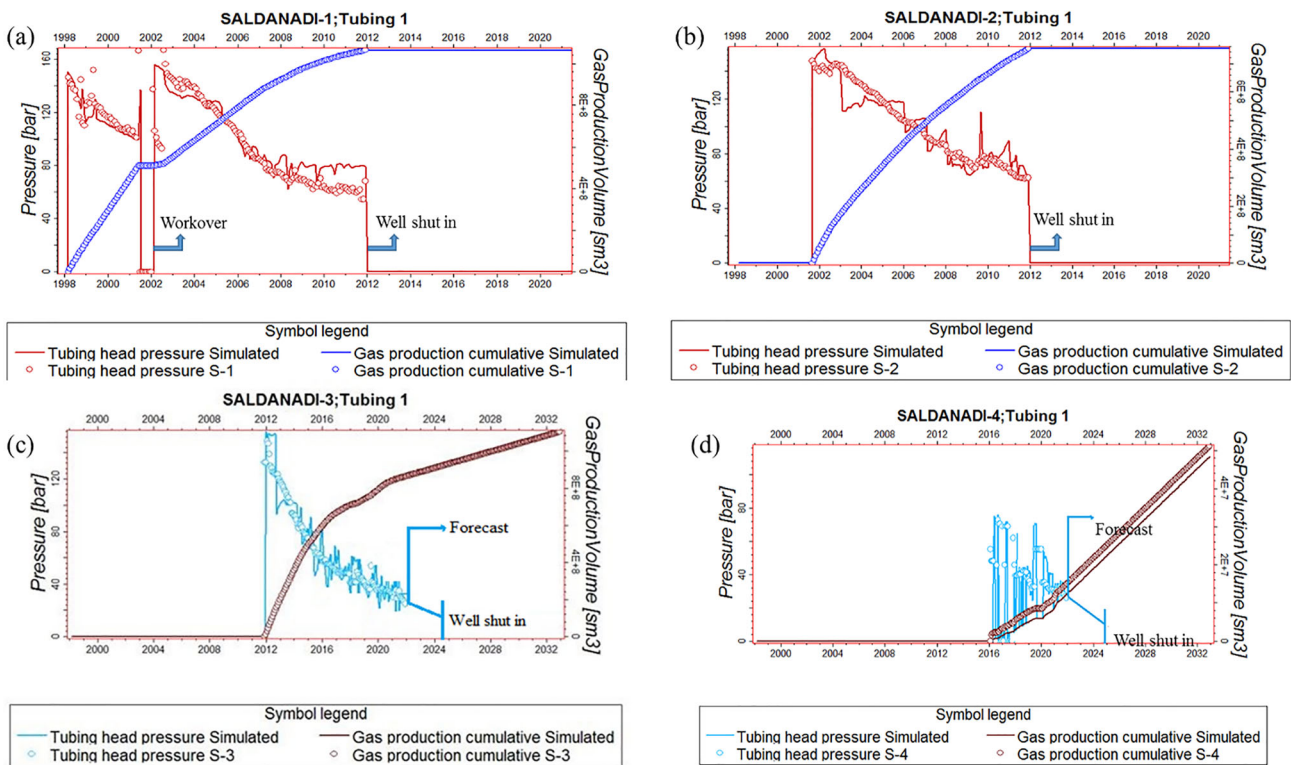


Figure 9. Wellhead pressure historical match (a) SLD #1, (b) SLD #2, (c) SLD #3 (with forecast), and (d) SLD #4 (with forecast).

Table 4. Depth intervals of reservoirs NGS 2, NGS 1, UGS and LGS of the Saldanadi gas field.

Well name	Depth interval (Measured depth)			
	New gas sand 2 (NGS 2)	New gas sand 1 (NGS 1)	Upper gas sand (UGS)	Lower gas sand (LGS)
SLD #1	1866–1913	2034–2063	2158–2260	2404–2429
SLD #2	1940–2010	2129–2163	2263–2373	2417–2447
SLD #3	2152–2228	2353–2384	2628–2657	2830–2880
SLD #4	2150–2227	2384–2426	2539–2633	2690–2755

Table 5. Volumetric calculation and gas initially in place (GIIP) estimation.

Gas sand	Bulk volume (10^6 sm^3)	Net volume (10^6 sm^3)	Pore volume (10^6 sm^3)	HCPV gas (10^6 sm^3)	GIIP (10^6 sm^3)	Cumulative production (sm^3)	Gas water contact (at tvdss)
NGS 2	258	171	32	25	4275	18.49×10^8	1897 m
NGS 1	207	127	21	17	2835		2021 m
UGS	518	326	48	38	6456		2215 m
LGS	121	80	10	8	1397		2411 m
Total GIIP = $149.63 \times 10^8 \text{ sm}^3$							

Table 6. Production forecasting and recovery factor estimation (no action).

Well no.	Well lifetime	Cumulative production, sm^3	Remaining gas reserve, sm^3	Gas initially in place (GIIP), sm^3	Ultimate recovery factor (RF)
SLD #1	Mar. 1998–Jan. 2012	1064433536	131.14×10^8	149.63×10^8	31.11%
SLD #2	Feb. 2002–Jan. 2012	751542144			
SLD #3	July 2021–Dec. 2024	2570984192			
SLD #4	July 2021–Nov. 2024	268608064			
Total production = $18.49 \times 10^8 \text{ sm}^3$					

4.3 Reservoir volumetric analysis

Hydrocarbon reserve estimation relies on petrophysical parameters, well-log data, core analysis, drill stem tests (DST), and reservoir modelling outputs through geostatistical methods. This study identified four potential gas sand zones, which is one more than previous studies. This addition has increased the estimated hydrocarbon reserves and holds significance for future well placement and field development strategies. The structural model and constructed petrophysical model are utilised after a static field model is produced to calculate the reservoir's reserves in terms of gas initially in place (Orellana *et al.* 2014). A volumetric calculation method is used to estimate the gas initially in place (GIIP), which is determined to be $149.63 \times 10^8 \text{ sm}^3$. The remaining reserve in the field is $131.14 \times 10^8 \text{ sm}^3$, and the cumulative production is reported in table 5.

4.4 Reservoir performance and forecasting

Dynamic modelling based on historical production profiles reveals the dynamic nature of the gas field. Wells SLD #1 and SLD #2 have ceased production due to low production rates, rapid tubing head pressure decline, and sand and water production issues. Wells SLD #3 and SLD #4 show a decline in the wellhead pressure and production rates, coupled with sand fragmentation during production. Sand particles clog the perforation, which reduces the permeability near the wellbore and the flow path of the gas. This gradually decreases the well production as well as the pressure. To address these issues, a skin effect is introduced to address the perforation damage during the historical match. Additionally, the issues could be due to a skin effect in the tubing or damage to the formation during drilling and/or completion.

A no-action situation is presented, i.e., continue gas production with the existing two wells (SLD #3 and SLD #4) without improving well or reservoir performance. Figure 9(c and d) shows the field's production profile for the no-action situation. The simulation predicts that production will cease by the end of 2024, with a shutdown pressure of 2.07 bar. The cumulative production is estimated to be approximately $18.49 \times 10^8 \text{ sm}^3$, with a recovery factor of 31.11% (table 6). Despite a 68.89% reserve, the rapid decline in production suggests the need for interventions to address potential wellbore damage or incorrect perforations. Therefore, it is essential to consider reservoir development and management strategies, such as drilling new infill wells and workovers of existing wells, to maximise recovery.

5. Conclusions

This research employed integrated geophysical, geological, and petrophysical interpretations utilising the sequential Gaussian simulation (SGS) method to distribute reservoir attributes and capture heterogeneities within potential gas sands. The overarching objective of this study was to utilise seismic and geophysical data to assess the structural characteristics, petrophysical properties, volumetric parameters, 3D distribution, history matching, and forecasting of the Saldanadi reservoir. Integrated datasets were pivotal in evaluating the reservoir's distribution and quality and mitigating uncertainties throughout the gas field's development process.

Through this comprehensive investigation, we identified four primary reservoir gas sands with varying thicknesses. The seismic-well tie between seismic and well-log signatures played a crucial role in this discovery. Historical data were meticulously analysed to gauge the reservoir's effectiveness and understand its dynamic behaviour. The 3D static reservoir model was validated by historical production and pressure data, ensuring the alignment of the simulated modelling through Eclipse software.

The updated model used in this study revealed a projected GIIP of $149.63 \times 10^8 \text{ sm}^3$, nearly $56.63 \times 10^8 \text{ sm}^3$ greater than the previous estimate, owing to the identification of additional potential gas-bearing sands. This revised model enhances prediction accuracy, enabling a more reliable understanding of the reservoir's static and dynamic behaviour under existing conditions. Based on simulations, it is expected that production from wells SLD #3 and SLD #4 will cease by the end of 2024, with a shutting pressure of

2.07 bar. Furthermore, the ultimate recovery factor for all four wells is estimated to be approximately 31.11%. This model is integral for defining prospective zones, determining suitable locations for new infill wells, and achieving the ultimate recovery factor. As a result, it is believed that forecasts based on this improved model will provide greater certainty and guide the next gas field development plan.

6. Recommendations

To further enhance our understanding of this reservoir, it is advisable to conduct a 3D seismic survey in the area. Such a survey would not only confirm the degree of reservoir continuity but also delineate the reservoir margins more clearly, facilitating the diagnosis of any issues. Additionally, consideration should be given to the development of additional infill wells, workovers, and potential hydraulic fracturing techniques to optimise the recovery factor and enhance overall reservoir performance. These measures will be pivotal in ensuring the efficient and sustainable development of the gas field.

Acknowledgements

The majority of the pertinent data used in this study effort are provided by Bangladesh Oil, Gas, and Mineral Corporation (Petrobangla) and Bangladesh Petroleum Exploration and Production Company Limited (BAPEX), for which the authors are grateful. Additionally, we appreciate the feedback from the reviewers and language editor, both of whom increased the quality of the paper.

Author statement

MAR: Conceptualization, data analysis, software, and original draft preparation. MAI: Methodology, software, and creative idea. JK: Data sorting, software, and creative ideas. ASDA: Writing, reviewing, and editing. MNAZ: Visualization, reviewing, and referencing. MYK: Visualization and reviewing.

References

Abd El-Gawad E A, Abdelwahhab M A, Bekiet M H, Noah A Z, Elsayed N A and Abd Elhamed E F 2019 Static reservoir modeling of El Wastani formation, for justifying

- development plans, using 2D seismic and well log data in Scarab field, offshore Nile Delta, Egypt; *J. Afr. Earth Sci.* **158** 103546, <https://doi.org/10.1016/j.jafrearsci.2019.103546>.
- Abdel-Fattah M, Dominik W, Shendi E, Gadallah M and Rashed M 2010 3D integrated reservoir modelling for upper safa gas development in Obaiyed field, Western Desert, Egypt; *72nd EAGE Conf. Exh. Inc. SPE EUROPEC 2010* cp-161-00766, <https://doi.org/10.3997/2214-4609.201401358>.
- Abdelmaksoud A and Radwan A 2022 Integrating 3D seismic interpretation, well log analysis and static modelling for characterising the Late Miocene reservoir, Ngatoro area, New Zealand; *Geomech. Geophys. Geo-Energ. Geo-Resour.* **8** 63, <https://doi.org/10.1007/s40948-022-00364-8>.
- Adelu A O, Aderemi A, Akanji A O, Sanuade O A, Kaka S I, Afolabi O, Olugbemiga S and Oke R 2019 Application of 3D static modeling for optimal reservoir characterisation; *J. Afr. Earth Sci.* **152** 184–196, <https://doi.org/10.1016/j.jafrearsci.2019.02.014>.
- Adeoti L, Onyekachi N, Olatinsu O, Fatoba J and Bello M 2014 Static reservoir modeling using well log and 3-D seismic data in a KN field, offshore Niger Delta, Nigeria; *Int. J. Geosci.*, <https://ir.unilag.edu.ng/handle/123456789/5341>.
- Ahmad N, Khan S and Al-Shuhail A 2021 Seismic data interpretation and petrophysical analysis of Kabirwala area Tola (01) well, Central Indus Basin, Pakistan; *Appl. Sci.* **11** 2911, <https://doi.org/10.3390/app11072911>.
- Alao P A, Olabode S O and Opeloye S A 2013 Integration of seismic and petrophysics to characterise reservoirs in ‘ALA’ oil field; *Sci. World J.* **10** 15, <https://doi.org/10.1155/2013/421720>.
- Ali A M, Radwan A E, Abd El-Gawad E A and Abdel-Latif A-SA 2022 3D Integrated structural, facies and petrophysical static modeling approach for complex sandstone reservoirs: A case study from the Coniacian–Santonian Matulla Formation, July Oilfield, Gulf of Suez, Egypt; *Nat. Resour. Res.* **31** 385–413, <https://doi.org/10.1007/s11053-021-09980-9>.
- Amanipoor H 2019 Static modeling of the reservoir for estimate oil in place using the geostatistical method; *Geod. Cartogr.* **45** 147–153, <https://doi.org/10.3846/gac.2019.10386>.
- Amigun J and Bakare N 2013 Reservoir evaluation of ‘Danna’ field Niger delta using petrophysical analysis and 3D seismic interpretation; *Pet. Coal.* **55** 119–127.
- Babu M N, Ambati V and Nair R R 2022 Lithofacies and fluid prediction of a sandstone reservoir using pre-stack inversion and non-parametric statistical classification: A case study; *J. Earth Syst. Sci.* **131** 55, <https://doi.org/10.1007/s12040-021-01792-y>.
- Bangladesh Oil G M C P 2009a Saldanadi Geological Study Report by RPS Energy Consultants Limited (RPS); *Petrobangla*, 33p.
- Bangladesh Oil G M C P 2009b Saldanadi Geophysics Report by RPS Energy prepared for Petrobangla; *Petrobangla*, 36p.
- Bangladesh Oil G M C P 2009c Saldanadi reservoir simulation study report by RPS Energy Consultants Limited (RPS); *Petrobangla*, 53p.
- Bangladesh Oil G M C P 2023 Petrobangla Production Report June 2023; *Petrobangla*, 15p.
- Bangladesh Petroleum Exploration P C B 2004 Well completion report on Saldanadi Well No. 1; *BAPEX*, 79p.
- Baouche R, Sen S, Debiane K and Ganguli S S 2020 Integrated reservoir characterisation of the Paleozoic and Mesozoic sandstones of the El Ouar field, Algeria; *J. Pet. Sci. Eng.* **194** 107551, <https://doi.org/10.1016/j.petrol.2020.107551>.
- Bapex B P E P C 2001a Geologging report of Saldanadi well-2; *BAPEX*, 9p.
- Bapex B P E P C L 2001b Re-evaluation of reserve of Saldanadi Gas Field; *BAPEX*, 33p.
- Cunha L 2003 Integrating static and dynamic data for oil and gas reservoir modelling; *Canadian Int. Pet. Conf. PET-SOC-2003-2219*, <https://doi.org/10.2118/2003-219>.
- Dey Deb P, Kanti P, Akhter Shireen and Debotosh 2016 Reserve estimation of Saldanadi Gas Field; *IJJAS* **16** 166–172.
- Du C, Zhang X, Melton B, Fullilove D, Sulimov B, Gowellly S, Grant D and Calvez J L 2009 A workflow for integrated Barnett shale gas reservoir modeling and simulation; *Latin American and Caribbean Pet. Eng. Conf.*, <https://doi.org/10.2118/122934-MS>.
- Ebong E D, Akpan A E, Ekwok S E, Esu E O and Ebong L A 2021 3-D reservoir characterisation and hydrocarbon volumetric estimation of parts of Niger Delta Basin-Nigeria; *J. Afr. Earth Sci.* **180** 104207, <https://doi.org/10.1016/j.jafrearsci.2021.104207>.
- Ehsan M and Gu H 2020 An integrated approach for the identification of lithofacies and clay mineralogy through Neuro-Fuzzy, cross plot and statistical analyses, from well log data; *J. Earth Syst. Sci.* **129** 101, <https://doi.org/10.1007/s12040-020-1365-5>.
- Ehsan M, Gu H, Ali A, Akhtar M M, Abbasi S S, Miraj M A F and Shah M 2021 An integrated approach to evaluate the unconventional hydrocarbon generation potential of the Lower Goru Formation (Cretaceous) in Southern Lower Indus basin, Pakistan; *J. Earth Syst. Sci.* **130** 90, <https://doi.org/10.1007/s12040-021-01584-4>.
- Elsheikh A, Setto I and Abdelhady A A 2021 Reservoir characterisation and 3D modeling of the Aptian Alamein Formation in North Razzak area (North Western Desert, Egypt); *J. Afr. Earth Sci.* **173** 104039, <https://doi.org/10.1016/j.jafrearsci.2020.104039>.
- Faleide T S, Braathen A, Lecomte I, Mulrooney M J, Midtkandal I, Bugge A J and Planke S 2021 Impacts of seismic resolution on fault interpretation: Insights from seismic modelling; *Tectonophysics.* **816** 229008, <https://doi.org/10.1016/j.tecto.2021.229008>.
- Ganguli S S 2017 Integrated reservoir studies for CO₂-enhanced oil recovery and sequestration: Application to an Indian mature oil field; *Springer*, pp. 99–115.
- Ganguli S S and Sen S 2020 Investigation of present-day in-situ stresses and pore pressure in the south Cambay Basin, western India: Implications for drilling, reservoir development and fault reactivation; *Mar. Pet. Geol.* **118** 104422, <https://doi.org/10.1016/j.marpetgeo.2020.104422>.
- Ganguli S S, Vedanti N, Akervoll I and Dimri V 2016 Assessing the feasibility of CO₂-enhanced oil recovery and storage in mature oil field: A case study from Cambay basin; *J. Geol. Soc. India.* **88** 273–280, <https://doi.org/10.1007/s12594-016-0490-x>.
- Ganguli S S, Vedanti N, Pandey O P and Dimri V P 2018 Deep thermal regime, temperature induced over-pressured zone and implications for hydrocarbon potential in the Ankleshwar oil field, Cambay basin, India; *J. Asian Earth Sci.* **161** 93–102, <https://doi.org/10.1016/j.jseaes.2018.05.005>.
- Ilozobhie A and Egu D 2019 Static and dynamic reservoir sands characterisation of an oil field in the Niger Delta from seismic and well log data; *Asian J. Appl. Sci. Technol.* **3** 112–125.

- Khan N and Rehman K 2019 Petrophysical evaluation and fluid substitution modeling for reservoir depiction of Jurassic Datta Formation in the Chanda oil field, Khyber Pakhtunkhwa, northwest Pakistan; *J. Pet. Explor. Prod. Tech.* **9** 159–176, <https://doi.org/10.1007/s13202-018-0513-9>.
- Khan H A, Zouaghi T, Iftekhar S, Khan M J and Irfan M 2019 Plio-Pleistocene stratigraphic sequences and depositional model using 3D seismic interpretation constrained by well logs in Central Graben, North Sea; *J. Earth Syst. Sci.* **128** 85, <https://doi.org/10.1007/s12040-019-1113-x>.
- Khan H A, Qadir S A, Khan M J, Siddiqui F H and Ahsan M S 2023 Modelling of geomorphological features of fluvial systems in Eromanga Basin and North Sea using 3D seismic attributes; *J. Earth Syst. Sci.* **132** 62, <https://doi.org/10.1007/s12040-023-02076-3>.
- Li B, Li L, Wen X-H and Sun T 2023 Bridging computational stratigraphy and reservoir simulation for geologically realistic high-resolution reservoir modeling; *SPE Res. Sim. Conf. USA*, <https://doi.org/10.2118/212244-MS>.
- Mirzadeh S, Chambers R, Carvajal G, Singh A, Maučec M, Knabe S, Al-Jasmi A and El Din I 2014 Reservoir simulation design strategy for next-generation multi-level assisted history matching; *IPTC 2014: Int. Pet. Tech. Conf.* cp-395-00312, <https://doi.org/10.3997/2214-4609-pdb.395.IPTC-17518-MS>.
- Mukherjee B and Sain K 2019 Prediction of reservoir parameters in gas hydrate sediments using artificial intelligence (AI): A case study in Krishna–Godavari basin (NGHP Exp-02); *J. Earth Syst. Sci.* **128** 199, <https://doi.org/10.1007/s12040-019-1210-x>.
- Nabawy B S and Shehata A M 2015 Integrated petrophysical and geological characterisation of the Sidi Salem–Wakar sandstones, off-shore Nile Delta, Egypt; *J. Afr. Earth Sci.* **110** 160–175, <https://doi.org/10.1016/j.jafrearsci.2015.06.017>.
- Narayan S, Singh R, Mohan A, Vivek K, Acharya P and Pal S K 2023 Delineation of thin and discrete sand reservoir facies from shale-dominated Kopili Formation (Middle to Late Eocene) using the post-stack seismic inversion and neural network algorithm: A case study from Assam Basin, India; *J. Earth Syst. Sci.* **132** 81, <https://doi.org/10.1007/s12040-023-02097-y>.
- Naseer M T 2023 Application of instantaneous spectral decomposition-based porosity simulations for imaging shallow-marine stratigraphic traps of Lower-Eocene carbonates sequences of Indus Basin, Onshore Pakistan; *J. Earth Syst. Sci.* **132** 22, <https://doi.org/10.1007/s12040-022-02039-0>.
- Okoli A E, Agbasi O E, Lashin A A and Sen S 2021 Static reservoir modeling of the eocene clastic reservoirs in the Q-field, Niger Delta, Nigeria; *Nat. Resour. Res.* **30** 1411–1425, <https://doi.org/10.1007/s11053-020-09804-2>.
- Orellana N, Caverro J, Yemez I, Singh V and Sotomayor De La Serna J 2014 Influence of variograms in 3D reservoir-modeling outcomes: An example; *Lead. Edge* **33** 890–902, <https://doi.org/10.1190/tle33080890.1>.
- Othman A A A, Fathy M, Othman M and Khalil M 2021 3D static modeling of the Nubia sandstone reservoir, gamma offshore field, southwestern part of the Gulf of Suez, Egypt; *J. Afr. Earth Sci.* **177** 104160, <https://doi.org/10.1016/j.jafrearsci.2021.104160>.
- Qadri S M T, Islam M A, Shalaby M R and Eahsan Ul Haque A K M 2017 Seismic interpretation and structural modelling of Kupe field, Taranaki Basin, New Zealand; *Arab. J. Geosci.* **10** 295, <https://doi.org/10.1007/s12517-017-3078-x>.
- Rahimi M and Riahi M A 2020 Static reservoir modeling using geostatistics method: A case study of the Sarvak Formation in an offshore oilfield; *Carbonates Evaporites* **35** 62, <https://doi.org/10.1007/s13146-020-00598-1>.
- Rao X, Xu Y, Liu D, Liu Y and Hu Y 2021 A general physics-based data-driven framework for numerical simulation and history matching of reservoirs; *Adv. Geo-Energy Res.* **5** 422–436, <https://doi.org/10.46690/ager.2021.04.07>.
- Sallam S, Ahmad M, Nasr M and Gomari S R 2015 Reservoir simulation for investigating the effect of reservoir pressure on oil recovery factor; *Int. Adv. Res. J. Sci. Eng. Technol.* **2** 875–882.
- Saravanavel J, Ramasamy S M, Palanivel K and Kumanan C J 2019 GIS based 3D visualisation of subsurface geology and mapping of probable hydrocarbon locales, part of Cauvery Basin, India; *J. Earth Syst. Sci.* **129** 36, <https://doi.org/10.1007/s12040-019-1307-2>.
- Sen S, Abioui M, Ganguli S S, Elsheikh A, Debnath A, Besssao M and Abdelhady A A 2021 Petrophysical heterogeneity of the early Cretaceous Alamein dolomite reservoir from North Razzak oil field, Egypt integrating well logs, core measurements and machine learning approach; *Fuel* **306** 121698, <https://doi.org/10.1016/j.fuel.2021.121698>.
- Shang X, Zhao H, Long S and Duan T 2021 A workflow for integrated geological modeling for shale gas reservoirs: A case study of the Fuling Shale Gas Reservoir in the Sichuan Basin, China; *Geofluids* **2021** 6504831, <https://doi.org/10.1155/2021/6504831>.
- Sharifi M, Kelkar M and Karkevandi-Talkhooncheh A 2021 A workflow for flow simulation in shale oil reservoirs: A case study in Woodford shale; *Adv. Geo-Energy Res.* **5** 365–375, <https://doi.org/10.46690/ager.2021.04.03>.
- Soleimani M and Jodeiri Shokri B 2015 3D static reservoir modeling by geostatistical techniques used for reservoir characterisation and data integration; *Environ. Earth Sci.* **74** 1403–1414, <https://doi.org/10.1007/s12665-015-4130-3>.
- Toqeer M, Ali A, Alves T M, Khan A, Zubair and Hussain M 2021 Application of model based post-stack inversion in the characterisation of reservoir sands containing porous, tight and mixed facies: A case study from the Central Indus Basin, Pakistan; *J. Earth Syst. Sci.* **130** 61, <https://doi.org/10.1007/s12040-020-01543-5>.
- Vo Thanh H and Lee K-K 2022 3D geo-cellular modeling for Oligocene reservoirs: A marginal field in offshore Vietnam; *J. Pet. Explor. Prod. Technol.* **12** 1–19, <https://doi.org/10.1007/s13202-021-01300-4>.

Springer Nature or its licensor (e.g. a society or other partner) holds exclusive rights to this article under a publishing agreement with the author(s) or other rightsholder(s); author self-archiving of the accepted manuscript version of this article is solely governed by the terms of such publishing agreement and applicable law.